Switching and charge-density-wave transport in $NbSe_3$. II. ac characteristics

R. P. Hall
AT&T Bell Laboratories, Murray Hill, New Jersey 07974-2070

A. Zettl
Department of Physics, University of California, Berkeley, California 94720
(Received 11 January 1988)

The phenomenon of switching is studied further in the lower charge-density-wave (CDW) state of $NbSe_3$ by measurements of ac conductivity. Switching CDW's are found to be dynamically overdamped when pinned, but underdamped when sliding. The results support a phase-slip interpretation of switching.

I. INTRODUCTION

This article is the second in a series of papers on the phenomenon of switching in $NbSe_3$.[1-3] The term "switching" refers to the threshold behavior of a charge-density wave (CDW).[4] In nonswitching CDW transport, the velocity of a CDW increases gradually as an applied electric field exceeds the threshold field E_T for CDW depinning.[5] In switching transport, the CDW velocity increases abruptly and often hysteretically. The resulting difference between I-V curves for switching and nonswitching CDW's is quite striking. A nonswitching I-V curve departs smoothly from Ohmicity at threshold, whereas a switching CDW displays one or several[6] steplike breaks.

The first paper in this series, paper I, discussed the dc characteristics of switching CDW's.[1] Paper I showed that besides abrupt depinning, switching CDW's are associated with another striking phenomenon: discontinuities in CDW current. Under the application of only a dc electric field, a switching CDW typically breaks up into a series of velocity-coherent domains that are separated by extremely narrow interface regions.[7] Even those CDW's that comprise a single current domain are only marginally stable against breakup into smaller domains.[1] Current domains are notable because they are absent from nonswitching CDW's, as well as from switching CDW's which are heated to temperatures that suppress switching. Current domains imply the existence of phase-slip centers between domains, where the CDW amplitude fluctuates at the interdomain beat frequency. Paper I argued that phase slippage and amplitude fluctuations provide a natural explanation of the dc characteristics of switching CDW's.

The dynamics of switching CDW's are explored further in this paper, by studying the response of both pinned and sliding CDW's to small ac electric fields. We show that when switching CDW's are pinned, their dynamics is equivalent to the dynamics of nonswitching CDW's; but when switching CDW's are depinned, their dynamics is quite different. We argue that the dichotomy between pinned and sliding CDW dynamics supports a phase-slip interpretation of switching. Thus our results and analysis emphasize that switching represents a unique regime of CDW motion, in which amplitude dynamics is as important as phase dynamics to a description of CDW sliding.

II. METHODS AND RESULTS

Measurements of ac conductivity were performed on single crystals of $NbSe_3$ or iron-doped $NbSe_3$.[6] Paper I describes the preparation and characteristics of the crystals used in these experiments. Only results on $NbSe_3$ are reported here, because results on iron-doped $NbSe_3$ are essentially identical. The ac conductivity of a sample was measured in either the presence or absence of a dc bias field. A voltage of the form

$$V = V_{dc} + V_{ac}\cos(\omega t) \tag{1}$$

was applied to the sample and the current response I_{ac} of the sample was detected synchronously using a phase-sensitive amplifier. At low frequencies, $10\ \text{Hz} \leq \omega/2\pi \leq 5$ MHz, a Hewlett-Packard HP-4192 impedance analyzer was used to make two- and four-probe measurements of the sample response. At higher frequencies, $4 \leq \omega/2\pi \leq 500$ MHz, a Hewlett-Packard HP-8754A network analyzer was used to make two-probe measurements. The ac test signal was 1.0 or 2.5 mV rms, for high and low frequencies, respectively, whereas threshold voltages for the onset of CDW sliding were 3–30 mV in a typical sample, at high and low temperatures, respectively. The dc bias voltage varied between zero and several times the sample threshold voltage.

Measurements were made at temperatures below 59 K, in the lower CDW state of $NbSe_3$. In principle, the response of a crystal consists of contributions from the upper ($T_c = 144$ K) and lower CDW states of $NbSe_3$, as well as from uncondensed electrons. However, at the frequencies and voltages applied in these experiments, the upper CDW state of $NbSe_3$ does not contribute to the total electronic current. Furthermore, the conductivity due to uncondensed electrons (measured at temperatures above 144 K) has no frequency dispersion. Therefore the ac conductivity of the lower CDW state is defined as

$$\sigma_{CDW}=I_{ac}/V_{ac}-\sigma_0 , \quad (2)$$

where σ_0 is the low-field dc conductivity of the crystal (due to uncondensed electrons).

The experimental setup permitted measurements of dc I-V curves and narrow-band noise spectra, in addition to measurements of ac conductivity. In order to make a connection with the results of paper I, Fig. 1 shows the (current-controlled) I-V characteristics of a switching crystal at high and low temperatures. At the higher temperature, 39 K, the response of the crystal is indistinguishable from the response of a nonswitching crystal. The I-V curve becomes smoothly nonlinear for bias currents exceeding 24 μA (corresponding to a threshold field of $E_T=41$ mV/cm), and narrow-band noise spectra show that the departure from Ohmicity is due to uniform depinning of the CDW throughout the crystal. But at the lower temperature, 24 K, the I-V curve is broken at two critical biases, $I_{c1}=206$ μA and $I_{c2}=242$ μA (corresponding to critical fields of $E_{c1}=328$ mV/cm and $E_{c2}=348$ mV/cm, respectively). The first break is produced by a region of steep negative differential resistance,[2,8] whereas the second break is marked by a sharp, hysteretic switch. The existence of two critical fields indicates that the CDW does not depin uniformly. Instead, the CDW forms two current domains and each domain depins separately. Narrow-band noise spectra confirmed the presence of two incommensurable noise fundamentals, and hence the existence of two independent current domains. The drastic change in the dc characteristics of this crystal between high and low temperatures is typical for switching crystals, but does not occur in nonswitching crystals.

In contrast to dc conductivity, the ac conductivity of a switching crystal does not change qualitatively between high and low temperatures, as long as the CDW remains pinned. Figure 2 shows the pinned, $V_{dc}=0$ conductivity of the same crystal at 47 and 24 K. At 47 K, the in-phase component of conductivity ($\mathrm{Re}\sigma_{CDW}$, open circles) is zero at low frequencies and increases monotonically with increasing frequency. The out-of-phase component ($\mathrm{Im}\sigma_{CDW}$, open triangles) is small but nonzero at low frequencies, increases until moderately high frequencies, and then decreases for frequencies past 200 MHz. A crossover frequency,[9] $\omega_c/2\pi=60$ MHz, defines the frequency above which $\mathrm{Re}\sigma_{CDW}$ exceeds $\mathrm{Im}\sigma_{CDW}$. The general shape of σ_{CDW} is described by the response of an overdamped harmonic oscillator. In particular, $\mathrm{Im}\sigma_{CDW}$ remains positive even at frequencies exceeding the crossover frequency by an order of magnitude.

Some relatively minor changes are apparent in the conductivity at 24 K (solid symbols). The crossover frequency has increased from 60 to 500 MHz, and the conductivity at the crossover frequency has increased from 2.25 to 5.25 mS. Also, the shape of σ_{CDW} has changed slightly. The slopes of $\mathrm{Re}\sigma_{CDW}$ and $\mathrm{Im}\sigma_{CDW}$ are flatter at low frequency and steeper near the crossover frequency. However, similar changes in the shape of $\sigma_{CDW}(\omega)$, and in the magnitudes of ω_c and $\sigma_{CDW}(\omega_c)$, are observed in nonswitching CDW's.[5] We have generally found that the pinned conductivities of switching and nonswitching CDW's are indistinguishable, whether at high or low temperatures.

Many of the similarities in the ac response of switching and nonswitching CDW's disappear when the CDW's begin to slide. Figure 3 shows the low-temperature conductivity of the crystal in Figs. 1 and 2 at three dc biases: a subthreshold bias, 186 μA, just below I_{c1}, and two sliding biases, 210 and 243 μA, just above I_{c1} and I_{c2}, respective-

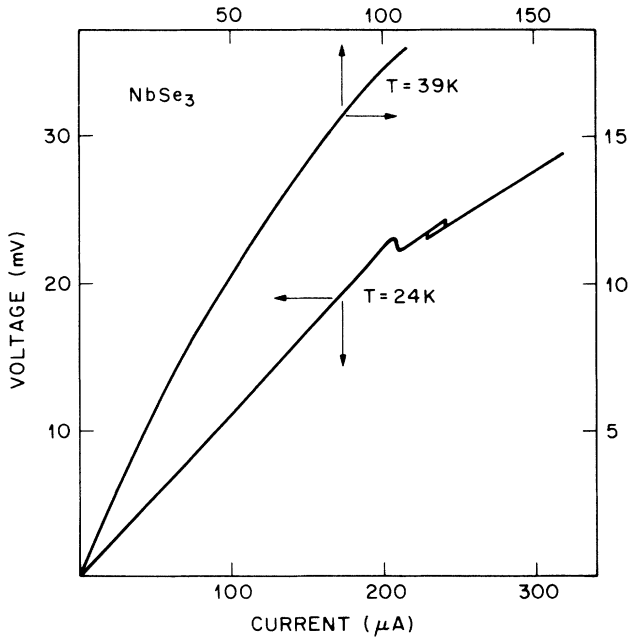

FIG. 1. Current-controlled I-V curves for a switching crystal of $NbSe_3$, at temperatures above (39 K) and below (24 K) the onset of switching.

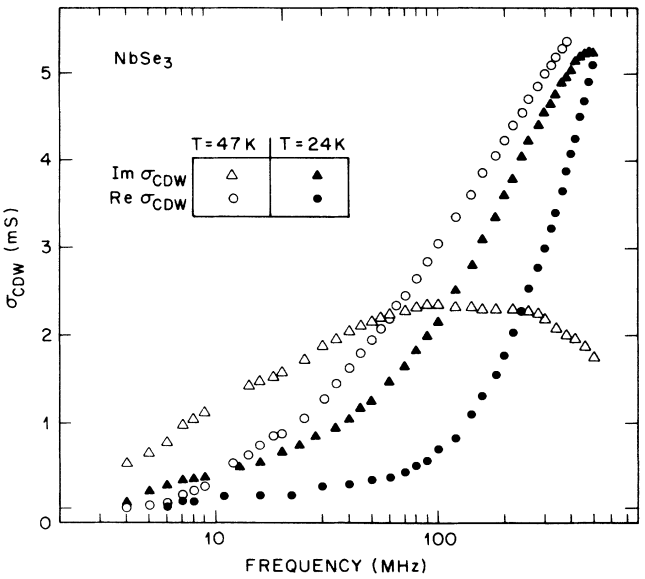

FIG. 2. The zero-bias, complex conductivity of the crystal in Fig. 1. Circles and triangles indicate the in-phase and out-of-phase components of conductivity, respectively. Open and solid symbols indicate data taken at 47 and 24 K, respectively.

ly. The subthreshold conductivity is identical to the conductivity in Fig. 2, but the sliding responses deviate substantially.

At high frequencies, differences between the pinned and sliding CDW responses are the least pronounced. In Fig. 3, the sliding response of the CDW asymptotically approaches the pinned response at frequencies above 200 MHz. The real component of conductivity approaches the pinned data from above, while the imaginary component approaches from below. As the dc bias increases, from 210 to 243 μA, convergence recedes to higher frequencies. Similar behavior is observed in the high-frequency behavior of nonswitching CDW's.[9] As discussed in Sec. III, the high-frequency convergence of pinned and sliding responses, both in switching and nonswitching CDW's, can be attributed to the effect of internal deformations of the CDW phase.[10]

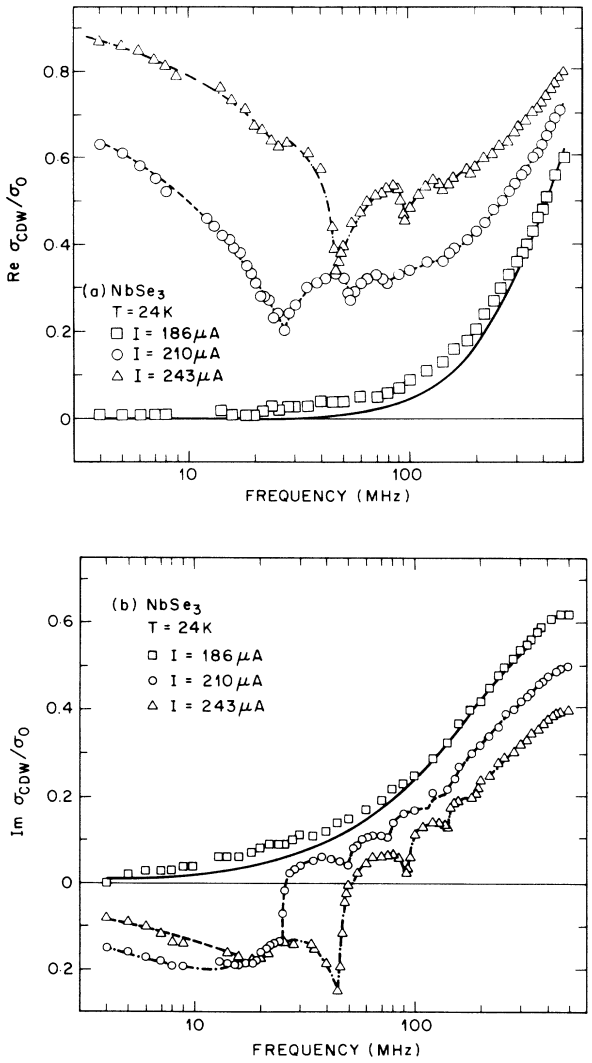

FIG. 3. (a) The in-phase component of conductivity at 24 K for the crystal from Fig. 1. The data are taken at three dc biases: just below the first break in the *I-V* curve of Fig. 1, just above the first break, and just above the second break. The lines are guides for the eye. (b) The out-of-phase component, taken at the same three dc biases.

At intermediate frequencies, the sliding conductivities in Fig. 3 are marked by a series of sharp interference features that occur when the ac frequency matches a narrow-band noise fundamental or one of its leading harmonics. With a current bias of 210 μA, interference effects occur at 27, 54, and 81 MHz due to the narrow-band noise associated with the first current domain that depins at 206 μA. With a current bias of 243 μA, the interference features that are prominent at 46, 92, and 138 MHz are again due to the first domain. In addition, a small feature occurs at 26 MHz due to the second current domain. (The narrow-band noise signal of the second current domain was much smaller than the signal of the first, which presumably explains why the interference effect produced by the second domain is so weak.) Interference effects also occur in nonswitching crystals,[9] although only one series of peaks is usually observed.

Differences between the pinned and sliding CDW responses are largest, both quantitatively and qualitatively, at frequencies below the narrow-band noise frequency. For example, $\mathrm{Re}\sigma_{CDW}$ in the pinned data is less than $0.03\sigma_0$ between 4 and 27 MHz, while $\mathrm{Re}\sigma_{CDW}$ in the 210-μA data begins at $0.60\sigma_0$ and then decreases by over 60%. Similarly, $\mathrm{Im}\sigma_{CDW}$ in the pinned data begins at zero and increases to $0.10\sigma_0$, while $\mathrm{Im}\sigma_{CDW}$ in the sliding data begins at $-0.15\sigma_0$ and decreases to $-0.20\sigma_0$ before slightly increasing again. At least for $\mathrm{Re}\sigma_{CDW}$, the difference between pinned and sliding conductivities at the lowest frequencies can be explained by the *I-V* curve in Fig. 1. The dc differential conductance of a CDW is the $\omega=0$ limit of ac conductivity. In Fig. 1, the conductance of the CDW at 210 μA is $0.67\sigma_0$, a value which is close to the observed value of $\mathrm{Re}\sigma_{CDW}$ at 4 MHz. But the other aspects of Fig. 3—the large dispersion in $\mathrm{Re}\sigma_{CDW}$ and the inductive behavior of $\mathrm{Im}\sigma_{CDW}$ over a decade in frequency—are quite striking and are without parallel in the conductivity of nonswitching CDW's.

In nonswitching CDW's, the sliding conductivity remains equal to the $\omega=0$ limit, $\mathrm{Re}\sigma_{CDW}=dI/dV-\sigma_0$ and $\mathrm{Im}\sigma_{CDW}\cong 0$, until just below the narrow-band noise frequency.[9] Inductive features are sometimes seen in nonswitching CDW's over narrow frequency ranges where the ac frequency matches the narrow-band noise frequency, but the features in Fig. 3 are much larger. To underscore the size of inductive features in switching crystals, Fig. 4 shows the conductivity of a second $NbSe_3$ crystal, measured at frequencies from 10 Hz to the narrow-band noise frequency of 1 MHz. Both $\mathrm{Re}\sigma_{CDW}$ and $\mathrm{Im}\sigma_{CDW}$ are reduced below their $\omega=0$ limits over very broad frequency ranges, three decades in frequency from 1 kHz to 1 MHz. These large, broad reductions in $\mathrm{Re}\sigma_{CDW}$ and $\mathrm{Im}\sigma_{CDW}$ are characteristic features in the conductivities of all the switching crystals that we have examined. We shall refer to these features as *inductive anomalies.*

The effect of inductive anomalies can be displayed in an alternative fashion by fixing the ac frequency and

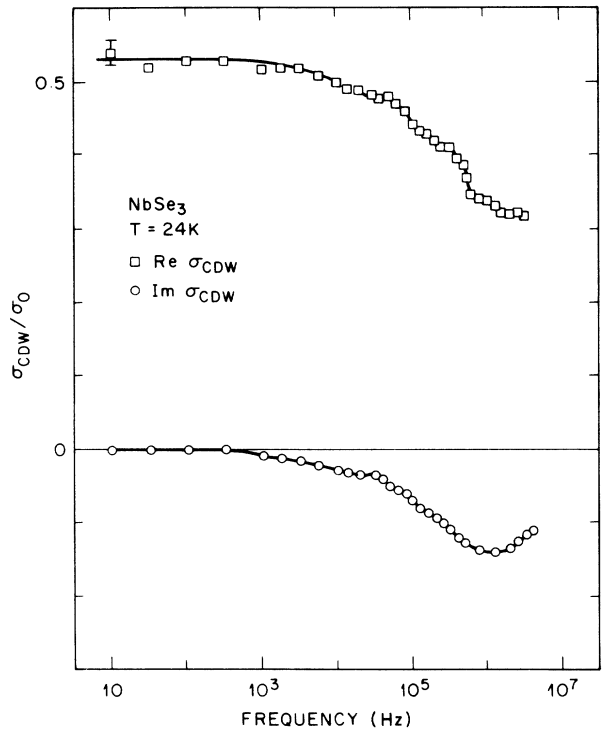

FIG. 4. The low-frequency, complex conductivity of a second switching crystal of $NbSe_3$, taken at a dc bias where the narrow-band noise frequency is about 1 MHz. The lines are guides for the eye.

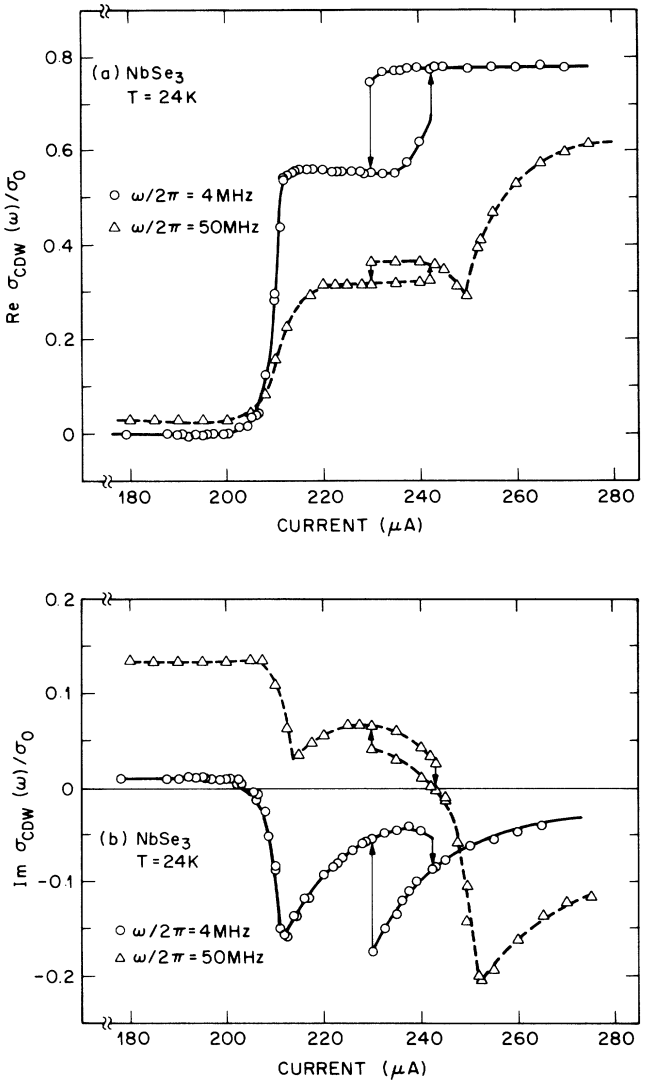

FIG. 5. (a) The in-phase conductivity, measured at 4 and 50 MHz, for the crystal from Fig. 1 as a function of dc bias. Except when the CDW is pinned, the 50-MHz conductivity is smaller than the 4-MHz conductivity. The lines are guides for the eye. (b) The out-of-phase conductivity as a function of dc bias.

sweeping the dc bias. Figure 5 shows the conductivity at 4 and 50 MHz for the crystal of Figs. 1–3. Two separate depinnings of the CDW, one by each current domain, are evident in the data for $Re\sigma_{CDW}$ and $Im\sigma_{CDW}$. Each depinning causes an abrupt increase in $Re\sigma_{CDW}$ and an abrupt decrease in $Im\sigma_{CDW}$. In addition, both $Re\sigma_{CDW}$ and $Im\sigma_{CDW}$ decrease as the narrow-band noise frequency (of the first current domain) approaches the frequency of the ac signal. This effect is observable only in the 50-MHz data, since narrow-band noise frequencies in this crystal are always well above 4 MHz because of switching. A striking feature of Fig. 5(a) is that the 4-MHz data are *larger* than the 50-MHz data when the CDW is depinned. The 50-MHz data exceed the 4-MHz data only when the CDW is pinned or when the current bias is much greater than 300 μA. In a nonswitching crystal, a conductivity measured at 50 MHz always exceeds a conductivity measured at 4 MHz, because the conductivity of a nonswitching CDW is a monotonically increasing function of ac frequency and dc bias. The inversion of conductivities in a switching CDW is produced by the unusual dispersion of inductive anomalies, in which CDW conductivity decreases with increasing frequency.

As a final observation, we comment briefly on the temperature dependence of inductive anomalies. Although we have observed inductive anomalies only in crystals that display switching, we have observed inductive anomalies at temperatures well above the onset of switching. For example, switching and hysteresis in one crystal were observed starting at temperatures below 30 K, but inductive anomalies were observed at temperatures as high as 42 K. Inductive anomalies are not unusual in this respect. Other phenomena connected with switching, such as a bistable low-field resistance[1] or a period-doubled response to ac signals,[2,11] are also observed above the onset of switching. In fact, all three phenomena are closely related by their dependence on a polarized CDW phase, as we shall explain in the next section and in paper III.[2]

III. ANALYSIS

CDW dynamics may be analyzed in terms of the classical, rigid-phase model of Grüner, Zawadowski, and Chaikin.[12] The model is relatively simple, possesses an intuitive physical interpretation, and qualitatively reproduces many aspects of the ac conductivity of nonswitching

CDW's. These advantages make the rigid-phase model a useful starting point for a discussion of the ac conductivity of switching CDW's.

The rigid-phase model treats the CDW amplitude as fixed and the CDW phase as uniform throughout a CDW conductor. The equation of motion is

$$\frac{d^2\phi}{dt^2}+\frac{1}{\tau}\frac{d\phi}{dt}+\omega_0^2 F(\phi)=\frac{e}{m^*}EQ \ , \tag{3}$$

where ϕ is the CDW phase, m^* is the effective CDW mass, Q is the CDW wave vector, and τ is a phenomenological time constant describing dissipation. The frequency ω_0 parametrizes the strength of CDW pinning, and the function $F(\phi)$ is a dimensionless pinning force. The pinning force is a periodic function of the CDW phase, and is usually approximated by its first Fourier component, $F(\phi)=\sin\phi$. Equation (3) may be rewritten in a dimensionless form,

$$\beta\ddot{\phi}+\dot{\phi}+F(\phi)=e_{\rm dc}+e_{\rm ac}\cos(\Omega t) \ , \tag{4}$$

where overdots represent differentiation with respect to time, which is measured in units of $(\omega_0^2\tau)^{-1}$. The frequency of the ac field is normalized to the corresponding unit of frequency, $\Omega=\omega/(\omega_0^2\tau)$, and the dc and ac field strengths are normalized to the threshold field: $e_{\rm dc}=E_{\rm dc}/E_T$ and $e_{\rm ac}=E_{\rm ac}/E_T$, where $E_T=m^*\omega_0^2/eQ$.

The remaining coefficient in Eq. (4) is the inertial parameter, $\beta=(\omega_0\tau)^2$. The inertial parameter is basically the time constant with which the CDW velocity approaches equilibrium. When β is zero or small, the CDW velocity is a deterministic function of the electric field and CDW phase, $\dot{\phi}=e-F(\phi)$. In this case, CDW dynamics is referred to as *overdamped*. When β is large, the CDW velocity lags behind the difference of the field and pinning forces, and CDW dynamics is called *underdamped*. In nonswitching crystals of $NbSe_3$, the inertial parameter is negligibly small and CDW dynamics is overdamped.[13] Typical numbers are $\tau=2.3\times10^{-12}$ s and $\omega_0=16$ GHz, which yield an inertial parameter of $\beta=1.4\times10^{-3}$. But in switching crystals, the magnitude (or even the relevance) of the inertial term is ambiguous. On one hand, Eq. (4) predicts switching and hysteresis[11,14] when $\beta\gtrsim1$, and analysis of the chaotic response in switching crystals leads to values of β that are as large as 2.1.[11] On the other hand, large values of β are grossly inconsistent with estimates of ω_0 and τ obtained from dc I-V characteristics.[1] In the analysis that follows, we shall compare the ac conductivity of switching CDW's to the ac conductivity of the underdamped and overdamped rigid-phase equations. We shall show that switching CDW's appear overdamped when pinned, but underdamped when sliding. We believe, however, that it is physically implausible to interpret our results in terms of phase inertia. Instead, we shall argue that phase slippage can mimic the effect of a motion-dependent inertia.

A. Pinned response

For ac signals of small amplitude, the pinned conductivity of Eq. (4) is equivalent to the response of a harmonic oscillator with a linear restoring force. When the applied bias is zero, the in-phase and out-of-phase components of conductivity are given, respectively, by

$$\begin{aligned}{\rm Re}\sigma(\Omega)&=\frac{ne^2\tau}{m^*}\frac{\Omega^2}{(1-\beta\Omega^2)^2+\Omega^2} \ ,\\ {\rm Im}\sigma(\Omega)&=\frac{ne^2\tau}{m^*}\frac{\Omega(1-\beta\Omega^2)}{(1-\beta\Omega^2)^2+\Omega^2} \ .\end{aligned} \tag{5}$$

Figure 6 shows these components as functions of the ac frequency. The curves in Fig. 6 define three characteristic frequencies:

$$\begin{aligned}\Omega_0&=\beta^{-1/2} \ ,\\ \Omega_\pm&=(\sqrt{1+4\beta}\pm1)/2\beta \ .\end{aligned} \tag{6}$$

The quantity Ω_0 is the normalized pinning frequency $\omega_0/\omega_0^2\tau$. The quantities $\Omega_\pm$ are the frequencies at which ${\rm Im}\sigma=\pm{\rm Re}\sigma$. For overdamped CDW's, Ω_- reduces to $\omega_0^2\tau$, which is called the crossover frequency, and Ω_+ reduces to the damping frequency τ^{-1}. The frequencies Ω_- and Ω_+ demarcate regimes of CDW response. For frequencies between 0 and Ω_-, CDW conductivity is mainly capacitive; between Ω_- and Ω_+, mainly dissipative; and between Ω_+ and ∞, mainly inductive.

As shown in Fig. 6, the inertial parameter may be determined directly from a measurement of ac conductivity, as long as measurement frequencies extend into the inductive regime of CDW conductivity. Measurements in the present experiments, such as in Fig. 2, were restricted to the capacitive regime of CDW response. However, the inertial parameter still may be determined, or at least bounded, by its effect on the shape of CDW conductivity. As the inertial parameter increases, the CDW conductivity flattens out at low frequencies and rises more steeply at frequencies approaching the crossover frequency Ω_-. This effect is shown in Fig. 7, where Eqs. (5) have been plotted for two values of the inertial

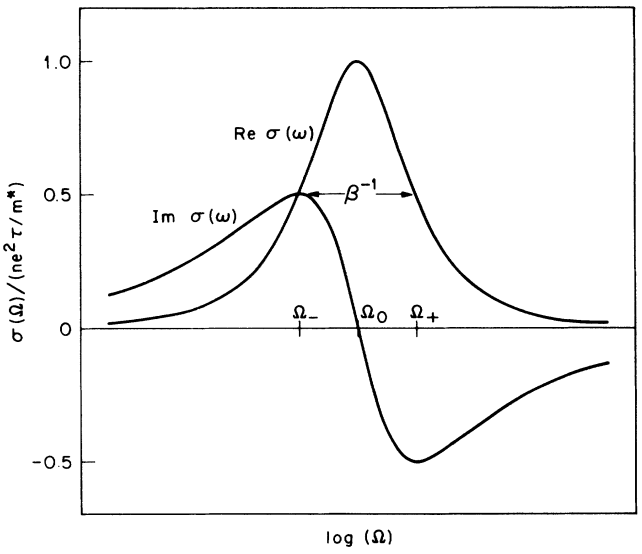

FIG. 6. The zero-bias pinned ac conductivity of the classical, rigid-phase of CDW dynamics [Eq. (4)].

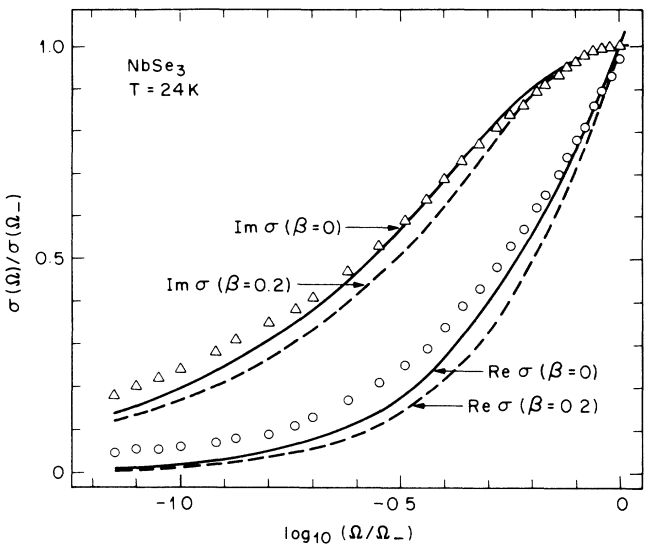

FIG. 7. The effect of the inertial parameter on the low-frequency, pinned conductivity of the rigid-phase model, for two values of the inertial parameter: $\beta=0$ and 0.2. The other parameters in the rigid-phase model are chosen so that the crossover frequency Ω_- is 500 MHz and the conductivity at the crossover frequency is $\sigma(\Omega_-)=5.25$ mS. The theoretical curves are superimposed on the 24-K data from Fig. 2.

parameter. The other parameters in Eqs. (5) have been adjusted so that Ω_- and $\sigma(\Omega_-)$, respectively, match the crossover frequency and conductivity of the 24-K data in Fig. 2, which are superimposed on the theoretical curves. Although neither the $\beta=0$ nor the $\beta=0.2$ curves fit the data in detail, the data are consistent with an overdamped inertial parameter somewhere in the range $0\leq\beta\leq 0.2$. Furthermore, as remarked earlier, the data are essentially identical to data measured on nonswitching crystals in this temperature range. Therefore, we conclude that switching CDW's, when pinned, are dynamically overdamped.

B. Sliding response

When the CDW slides in Eq. (4), the dc-induced narrow-band noise frequency Ω_N replaces the frequencies $\Omega_\pm$ as a characteristic frequency of CDW dynamics. In the context of Eq. (4), the narrow-band noise frequency is usually referred to as the *washboard frequency*. It is equal to the reciprocal of the time-averaged phase velocity in Eq. (4), $\Omega_N=\langle\dot{\phi}\rangle^{-1}$. For ac frequencies below or far above the washboard frequency, the ac conductivity of a sliding CDW may be calculated perturbatively. At frequencies below the washboard frequency, the main effect of an ac test signal is to produce a slow modulation of the dc bias. Therefore the ac conductivity is closely related to the dc differential conductivity of the CDW:

$$\mathrm{Re}\sigma(\Omega)=\frac{ne^2\tau}{m^*}\frac{d\langle\dot{\phi}\rangle}{de}[1-(\beta\Omega)^2]\ ,$$
$$\mathrm{Im}\sigma(\Omega)=-\frac{ne^2\tau}{m^*}\frac{d\langle\dot{\phi}\rangle}{de}(\beta\Omega)\ . \tag{7}$$

The prefactor $(ne^2\tau/m^*)d\langle\dot{\phi}\rangle/de$ is the slope of the (voltage-controlled) I-V curve. As a function of frequency, the real component of conductivity starts at dI/dV and decreases quadratically with increasing frequency. The imaginary component starts at zero and decreases linearly. The rate of decrease for both Reσ and Imσ is set by the inertial parameter. For overdamped CDW's, in which β is small, reductions in Reσ and Imσ are negligible.[15] For underdamped CDW's, in which $\beta\Omega$ can approach 1, reductions in Reσ and Imσ are appreciable and in fact resemble the inductive anomalies that characterize the sliding conductivity of switching CDW's.

At ac frequencies above the washboard frequency and its leading harmonics, the role of the ac and dc signals in Eq. (4) is reversed. The dc signal now produces a slow variation of the potential tested by the ac signal, and therefore the CDW conductivity is given by

$$\sigma(\Omega)=\frac{ne^2\tau}{m^*}\frac{i\Omega}{[(i\Omega-\beta\Omega^2)^2-1]^{1/2}}\ .$$

For overdamped CDW's the limit $1\ll\Omega\ll\beta^{-1}$ is relevant. To order Ω^{-2}, the CDW conductivity reduces to

$$\mathrm{Re}\sigma(\Omega)=\frac{ne^2\tau}{m^*}(1-\tfrac{1}{2}\Omega^{-2})\ ,$$
$$\mathrm{Im}\sigma(\Omega)=0\ . \tag{8}$$

The sliding conductivity of an overdamped CDW is essentially constant and in phase with the test signal at high frequencies. For underdamped CDW's the limit $\beta\Omega\gg 1$ is relevant, and the CDW conductivity reduces to

$$\mathrm{Re}\sigma(\Omega)=\frac{ne^2\tau}{m^*}(\beta\Omega)^{-2}$$
$$\mathrm{Im}\sigma(\Omega)=-\frac{ne^2\tau}{m^*}(\beta\Omega)^{-1}\ . \tag{9}$$

The sliding conductivity of an underdamped CDW quickly approaches zero at high frequencies.

At ac frequencies that are comparable to the washboard frequency or its harmonics, an ac signal interacts nonlinearly with the sliding motion of a CDW. In addition, ac-induced oscillations of the CDW are difficult to separate from the dc-induced narrow-band noise. Rather than calculate ac conductivities in this frequency range, we have used instead an analog computer (Philipp-Gillette JA-100) to simulate Eq. (4) and to measure conductivities directly. The simulated measurements are identical to the experimental measurements in Sec. II. A small ac signal is applied to the analog and the analog response is measured synchronously with a phase-sensitive detector. As with the experimental measurements, the simulated measurements do not distinguish between ac- and dc-induced oscillations of the CDW. The measurement procedure is equivalent to defining conductivity in Eq. (4) as

$$\sigma(\Omega)=\frac{ne^2\tau}{m^*}\frac{\tilde{\phi}(\Omega)}{e_{\mathrm{ac}}}\ ,$$

where $\tilde{\phi}(\Omega)$ is the Fourier component of the CDW phase velocity at the applied frequency.

Figures 8(a) and 8(b) show the results of analog simulations appropriate to overdamped and underdamped dynamics, respectively. In Fig. 8(a), the fitting parameters of Eq. (4) were chosen to be $\omega_0^2\tau/2\pi=500$ MHz and $\beta=0.005$, values which are consistent with the pinned ac conductivity in Fig. 7. In Fig. 8(b), the fitting parameters were chosen to be $\omega_0^2\tau/2\pi=22$ MHz and $\beta=2.1$, values which are suggested by Shapiro step and hysteresis experiments on $NbSe_3$.[11] In both figures, the dc bias was adjusted so that the narrow-band noise frequency was comparable to the noise frequencies in Fig. 3.

The results in Fig. 8 agree with the results of Eqs. (7)–(9). At low frequencies, $\mathrm{Re}\sigma(\Omega)$ decreases quadratically from dI/dV and $\mathrm{Im}\sigma(\Omega)$ decreases linearly from zero. The rate of decrease is set by β, so reductions in $\mathrm{Re}\sigma$ and $\mathrm{Im}\sigma$ are negligible in Fig. 8(a), where β is small, and appreciable in Fig. 8(b), where β is large. [In Fig. 8(a), the increase in $\mathrm{Re}\sigma$ just before the washboard frequency is due to mode locking between the ac and washboard frequencies.[15]] At high frequencies, the behavior of $\sigma(\Omega)$ depends on whether the CDW is underdamped or overdamped. For the overdamped calculation, $\mathrm{Re}\sigma$ attains the high-field, high-frequency limit of $ne^2\tau/m^*$, while $\mathrm{Im}\sigma$ is identically zero. For the underdamped calculation, $\mathrm{Re}\sigma$ rolls off as Ω^{-2}, while $\mathrm{Im}\sigma$ decreases as $-\Omega^{-1}$. At intermediate frequencies, both the underdamped and overdamped conductivities display a series of large interference peaks where the test frequency matches the washboard frequency or its harmonics.

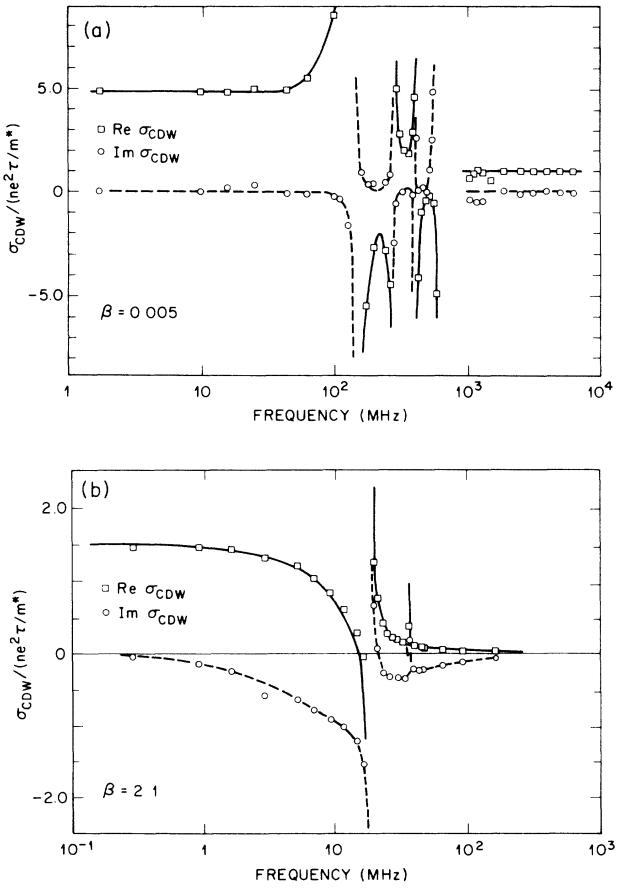

FIG. 8. (a) The sliding ac conductivity of the over-damped rigid-phase model, $\beta=0.0005$. The lines are guides for the eye. (b) The sliding ac conductivity of the underdamped rigid-phase model, $\beta=2.1$. The lines are guides for the eye.

The sliding ac conductivity of the rigid-phase model—whether underdamped or overdamped—obviously does not agree with the experimental data on switching CDW's. The model also does not agree with experimental data on nonswitching CDW's.[10] Three discrepancies are notable.

1. In the rigid-phase model, $\mathrm{Re}\sigma$ is larger at low frequencies than at high frequencies. In experiment, just the opposite behavior is observed: $\mathrm{Re}\sigma$ is smaller at low frequencies than at high frequencies.

2. At high frequencies in the rigid-phase model, $\mathrm{Im}\sigma$ is zero, but in experiment, $\mathrm{Im}\sigma$ approaches its pinned value.

3. Interference effects are much larger in the rigid-phase model than they are in experiment.

These discrepancies, however, can be traced to the model's assumption of a rigid CDW phase. Better results are obtained if the CDW phase is treated as deformable.[10] Fukuyama and Lee showed that a deformable CDW breaks up into a series of phase-coherent domains.[16] Within a domain, the CDW phase is fairly rigid. The dynamics of an individual domain may be modeled by Eq. (4) if an elastic coupling of the CDW phase to neighboring domains is included.[17]

Application of an electric field to a deformable CDW not only produces sliding motion of the CDW, but also internal motion of the CDW domains with respect to one another. The internal modes of a deformable CDW have three effects on its dynamics. First, the slope dI/dV of the dc I-V curve is reduced below the high-field limit $ne^2\tau/m^*$.[18] Consequently, $\mathrm{Re}\sigma$ becomes smaller at low frequencies than at high frequencies. Second, internal modes dominate the CDW response at high frequencies.[10] Therefore, $\mathrm{Im}\sigma$ approaches its high-frequency, pinned value even when a CDW is sliding. Third, internal modes reduce the size of the narrow-band noise signal.[18] This in turn reduces the interference features in $\sigma(\Omega)$ to a size which is consistent with experiment.

While improving agreement with the low-frequency limit of $\mathrm{Re}\sigma$, the high-frequency limit of $\mathrm{Im}\sigma$, and the size of interference features, a deformable CDW phase does not account for the inductive anomalies that are characteristic of switching CDW's. Discounting the discrepancies caused by the rigid-phase assumption, Eqs. (5) and Fig. 8 show that inductive anomalies are indicative of a CDW phase velocity that lags behind the applied ac signal. (The literature contains no underdamped, deformable-phase calculations of ac conductivity; therefore we cannot compare our experimental results with theoretical curves.) However, it is unlikely that the lag in CDW response is literally caused by phase inertia, only that the lag can be modeled by inertia. Phase inertia is an unappealing explanation of the CDW response for several reasons. As paper I points out, the origin of inertia would be difficult to explain in switching crystals. Furth-

ermore, phase inertia would have to depend on CDW motion in a peculiar manner. Because the CDW response is overdamped when pinned but underdamped when sliding, a hypothetical inertia would have to appear whenever a CDW started to slide. On the other hand, a velocity-dependent inertia would be evident in the high-frequency response of a pinned CDW, since the rms velocity of a CDW increases as the ac frequency increases. Because there is no evidence for an underdamped pinned mode, a hypothetical inertia would have to depend on the sliding motion of a CDW without depending on the CDW velocity. With such a complicated dependence on CDW motion, phase inertia does not provide a natural explanation for the underdamped response of switching CDW's.

C. Phase slippage

This section will argue that phase slippage can explain the ac characteristics of switching CDW's. To summarize the model presented in paper I, switching crystals are distinguished from nonswitching crystals by the presence of a small member of strong- (or "ultrastrong"-) pinning sites. Strong-pinning sites, which are present in addition to the weak impurities found in nonswitching crystals, nucleate the phase-slip centers that enable a switching CDW to slide. Strong-pinning sites produce large gradients in the CDW phase when an electric field is applied to a crystal. Polarization of the CDW phase leads to collapse of the CDW amplitude as the electric field increases.[3] When the amplitude collapses, the phase slips by a factor of 2π to relieve polarization. Then the amplitude reforms, phase polarization reaccumulates, and the phase-slip cycle repeats as the CDW amplitude collapses again. Each cycle of the phase-slip process advances the CDW phase by a factor of 2π.

Phase slippage causes switching when the polarization that accumulates at strong-pinning centers is very large.[3,19] A large polarization of the CDW phase is not relieved appreciably by a single phase-slip event; therefore the CDW amplitude reforms only partially during the phase-slip cycle. The elasticity of the phase depends on the CDW amplitude, and in turn the pinning of a CDW depends on phase elasticity. As a result, CDW pinning is restored only partially during each phase-slip cycle, and the effective collapse in pinning produces switching. When a CDW is pinned, its amplitude does not fluctuate and phase elasticity restrains motion of the CDW. When the CDW begins to slide, phase elasticity is reduced and the CDW velocity jumps from zero to a large value.

The phase-slip model explains the $\omega=0$ limit of ac conductivity, since it accounts for the shape of the dc dI/dV curve in switching crystals.[1] The phase-slip model may be extrapolated to finite frequencies by considering separately the cases of pinned and sliding CDW's. For the case of a pinned CDW, the interactions that determine the ac response of a switching CDW are the same as those for a nonswitching CDW. In a nonswitching CDW, phase domains respond to an ac signal like a collection of overdamped oscillators coupled together by the elasticity of the CDW phase. In a switching CDW, the only difference is the additional presence of strong-pinning sites. But the phase is essentially fixed at strong-pinning sites, because pinning frequencies there are comparable to the Peierls gap frequency. Therefore, strong-pinning interactions do not contribute to the ac response of a CDW for frequencies below the far infrared. Furthermore, because of their small number, strong-pinning sites do not appreciably reduce the oscillator strength of weak impurities. Therefore the pinned conductivity of switching CDW's should be nearly identical to the response of nonswitching CDW's.

For the case of a switching CDW, phase slippage produces a delayed motion of the CDW phase that has no counterpart in nonswitching CDW's. In order for the phase to advance in a switching CDW, the abrupt phase changes that occur at phase-slip centers must diffuse from the centers into the bulk of neighboring phase domains. The time required for a 2π change of phase to diffuse across a domain is on the order of the phase relaxation time. In the overdamped rigid-phase model, the relaxation time is given by $(\omega_0^2\tau)^{-1}$, or by $\beta=1$ in normalized units. When an ac signal is applied to a switching crystal, the phase diffusion time produces a delay between advances of the CDW phase and the maximum field of the ac cycle. Therefore the CDW velocity lags behind the ac signal with a time constant of $\beta\sim 1$. The lag has exactly the same effect that a phase inertia would have, and produces inductive anomalies in the ac response of the crystal. Because phase slippage occurs only when a CDW slides, inertialike effects are present only in the sliding, and not in the pinned, CDW state.

Significantly, switching and hysteresis are not required in the dc characteristics of a crystal in order for inertial effects to be present in its ac response. Switching and hysteresis require special conditions of phase polarization and impurity concentrations, but inertial effects require only phase slippage. This explains why inductive anomalies are observed in the ac response of a crystal at temperatures above the complete onset of switching.

IV. SUMMARY

We have presented the results of ac-conductivity measurements on switching crystals of $NbSe_3$. At temperatures well above the onset of switching, the ac response of switching and nonswitching crystals is equivalent. At temperatures below the onset of switching, the ac response of switching and nonswitching crystals is distinguishable only when the CDW's within the crystals are sliding. The sliding ac conductivity in switching crystals is marked by inductive anomalies, which are broad dips in $\mathrm{Re}\sigma_{\mathrm{CDW}}(\omega)$ and $\mathrm{Im}\sigma_{\mathrm{CDW}}(\omega)$ at frequencies below the narrow-band noise frequency. We have analyzed the ac response of switching crystals in terms of the rigid-phase model, which is the simplest differential equation of CDW transport. Although the data are not described in detail by this model, the model does show that switching CDW's are overdamped when pinned and underdamped

when sliding. We have argued that inertial effects in the sliding state arise from the same phase-slip mechanism that produces bistability and hysteresis in dc I-V curves. Thus phase slippage provides a self-consistent explanation of the ac and dc characteristics of switching CDW transport.

ACKNOWLEDGMENTS

This work was supported by National Science Foundation Grant No. DMR-84-00041. One of us (A.Z.) acknowledges support from the Alfred P. Sloan Foundation. The work of one of us (R.P.H.) was done at the University of California at Berkeley.

[1]R. P. Hall, M. F. Hundley, and A. Zettl, preceding paper, Phys. Rev. B **38**, 13 002 (1988).
[2]M. S. Sherwin, R. P. Hall, and A. Zettl, following paper, Phys. Rev. B **38**, 13 028 (1988).
[3]M. Inui, R. P. Hall, S. Doniach, and A. Zettl, this issue, Phys. Rev. B **38**, 13 047 (1988).
[4]A. Zettl and G. Grüner, Phys. Rev. B **26**, 2298 (1982).
[5]For a review of CDW transport, see G. Grüner and A. Zettl, Phys. Rep. **119**, 117 (1985).
[6]M. P. Everson and R. V. Coleman, Phys. Rev. B **28**, 6659 (1984).
[7]R. P. Hall, M. F. Hundley, and A. Zettl, Phys. Rev. Lett. **56**, 2399 (1986).
[8]R. P. Hall, M. S. Sherwin, and A. Zettl, Phys. Rev. Lett. **52**, 2293 (1984).
[9]A. Zettl and G. Grüner, Phys. Rev. B **25**, 2081 (1982).
[10]L. Sneddon, Phys. Rev. Lett. **52**, 65 (1984).
[11]R. P. Hall, M. S. Sherwin, and A. Zettl, Phys. Rev. B **29**, 7076 (1984).
[12]G. Grüner, A. Zawadowski, and P. M. Chaikin, Phys. Rev. Lett. **46**, 511 (1981).
[13]S. Sridhar, D. Reagor, and G. Grüner, Phys. Rev. Lett. **55**, 307 (1985).
[14]D. E. McCumber, J. Appl. Phys. **39**, 3113 (1968); W. C. Stewart, Appl. Phys. Lett. **12**, 277 (1968).
[15]P. S. Hagan and D. S. Cohen, J. Appl. Phys. **50**, 5408 (1979); H. Kanter and F. L. Vernon, *ibid.* **43**, 3174 (1972).
[16]H. Fukuyama and P. A. Lee, Phys. Rev. B **17**, 535 (1978).
[17]L. Pietronero and S. Strässler, Phys. Rev. B **28**, 5863 (1983); S. N. Coppersmith and D. S. Fisher, *ibid.* **28**, 2566 (1983); P. B. Littlewood, *ibid.* **33**, 6694 (1986).
[18]D. S. Fisher, Phys. Rev. B **31**, 1396 (1985); L. Sneddon, *ibid.* **29**, 725 (1984).
[19]R. P. Hall, M. F. Hundley, and A. Zettl, Physica **143B**, 152 (1986).